



LAWRENCE  
LIVERMORE  
NATIONAL  
LABORATORY

# On The Transient Space Localization Model

C. A. Iglesias

May 31, 2022

High Energy Density Journal

## **Disclaimer**

---

This document was prepared as an account of work sponsored by an agency of the United States government. Neither the United States government nor Lawrence Livermore National Security, LLC, nor any of their employees makes any warranty, expressed or implied, or assumes any legal liability or responsibility for the accuracy, completeness, or usefulness of any information, apparatus, product, or process disclosed, or represents that its use would not infringe privately owned rights. Reference herein to any specific commercial product, process, or service by trade name, trademark, manufacturer, or otherwise does not necessarily constitute or imply its endorsement, recommendation, or favoring by the United States government or Lawrence Livermore National Security, LLC. The views and opinions of authors expressed herein do not necessarily state or reflect those of the United States government or Lawrence Livermore National Security, LLC, and shall not be used for advertising or product endorsement purposes.

# On the transient space localization model

CARLOS A. IGLESIAS

*Lawrence Livermore National Laboratory  
P.O. Box 808, Livermore, CA 94550, USA*

## **Abstract**

Significant discrepancies relevant to helioseismology between experimental and theoretical photon absorption by plasmas remain unresolved. Interestingly, a new process called transient space localization (TSL) where the plasma perturbs the final state in photon ionization transitions purportedly enhances the cross-sections and resolves the extant discrepancies. It is found, however, that as described the TSL model leads to unphysical divergences. Furthermore, a minor but plausible modification to create a realizable TSL model can only increase the photon ionization cross-sections by at most 5%. Moreover, and contrary to the claims, for very strongly coupled plasmas it reduces the photon ionization cross-sections.

## 1. Introduction

Plasma radiative properties are integral to the study of high energy density physics in astrophysics, inertial and magnetic confinement, and warm dense matter. To test photon absorption models at extreme matter conditions, an experimental platform was developed at the Sandia Z Facility and theoretical results were in good agreement with the first measurements<sup>1</sup>. Unexpectedly, later experiments<sup>2</sup> at denser and hotter plasma conditions reported significantly larger photon absorption than predicted by theory. The enhanced opacity is welcomed by solar models<sup>3</sup>. The situation became more perplexing when a systematic study of the opacity dependence on atomic number did not produce as large differences with theory<sup>4</sup>.

Several efforts have examined the photon absorption models but so far failed to resolve the discrepancies<sup>5-13</sup>. Alternatively, these are challenging measurements and experimental errors could exist<sup>14</sup>. Most recently, the transient space localization (TSL) model was proposed as an explanation for the increased photon absorption<sup>15</sup>. The phenomenon has electrons in the final continuum states colliding with the plasma altering the usual distorted wave approach. The altered wavefunctions are claimed to enhance the photon ionization cross-sections and provide better agreement with the empirical results<sup>15,16</sup>.

The present goal is to assess fundamental aspects of the TSL model. The standard formulation of photon ionization with energy eigenstates is briefly reviewed in Section 2. It recalls basic concepts needed for the analysis of the TSL model presented in Sections 3. Conclusions are offered in the last Section 4.

## 2. Distorted wave approach

In linear response theory the rate of energy absorbed by a system from an external field is provided by the fluctuation-dissipation theorem<sup>17</sup>. The quantity of interest here is the line shape function for photon absorption by a plasma, which is given by

$$S(\omega) = \sum_{\alpha\beta} \rho_{\alpha} |\Phi_{\alpha\beta}|^2 \delta(\varepsilon_{\beta} - \varepsilon_{\alpha} - \hbar\omega) \quad (2.1)$$

where the sums are over the plasma initial and final stationary states  $\alpha$  and  $\beta$  with energies  $\varepsilon_{\alpha}$  and  $\varepsilon_{\beta}$ , respectively,  $\rho_{\alpha}$  is the probability of the system being in initial state  $\alpha$ ,  $\Phi_{\alpha\beta}$  is the matrix element for the interaction of the system with a photon, and an energy conserving  $\delta$ -function. For final continuum states an integral over energy with a density of states replaces the sum over  $\beta$ .

The line shape function represents the absorption spectrum as transitions between stationary energy eigenstates of the plasma in the absence of the external field. It is emphasized that within linear response theory Eq. (2.1) is an exact result. Practical calculations, however, require approximations since there is no known solution to the many-body problem. Here, an approximation is introduced to treat atomic processes in the plasma. That formulation leads to the standard distorted wave approach used by most photon absorption plasma models.

### 2.1 One-electron picture

Following the TSL treatment<sup>15</sup>, the description reduces the theory to a single active electron in an effective spherically symmetric Hamiltonian described by the mean field of the remaining bound electrons, nucleus located at the origin of the coordinate system, and the plasma. In addition, spin and relativistic effects are nonessential to the analysis and are neglected here to simplify notation.

In this picture, the energy and angular momentum eigenstate for an electron at spatial position  $\vec{r}$  at time  $t$  can be expressed in the form<sup>18</sup>

$$\psi_{\nu\ell m}(\vec{r}, t) = r^{-1} P_{\nu\ell}(r) Y_{\ell m}(\hat{r}) e^{-i\epsilon t/\hbar} \quad (2.1.1)$$

where  $r = |\vec{r}|$  and  $\hat{r}$  is a unit vector in the direction of  $\vec{r}$ ,  $\ell$  and  $m$  are respectively the orbital angular momentum and magnetic quantum numbers, and  $Y_{\ell m}(\hat{r})$  is a spherical harmonic. The reduced wavefunctions satisfy the radial Schrodinger equation,

$$\left\{ -\frac{\hbar^2}{2\mu} \left[ \frac{d^2}{dr^2} + \frac{\ell(\ell+1)}{r^2} \right] + V(r) - \epsilon \right\} P_{\nu\ell}(r) = 0 \quad (2.1.2)$$

with  $\mu$  the electron reduced mass and  $V(r)$  a model dependent central potential vanishing at large radius. For bound states with  $\epsilon < 0$ ,  $\nu$  denotes the principal quantum number  $n$ . For continuum states  $\nu = \epsilon > 0$ . The boundary condition at the origin is

$$P_{\nu\ell}(r \rightarrow 0) \propto r^{\ell+1} \quad (2.1.3)$$

The boundary conditions at infinity are

$$P_{\nu\ell}(r \rightarrow \infty) \propto \begin{cases} 0 & , \text{ bound state} \\ \cos(qr + \delta) & , \text{ continuum state} \end{cases} \quad (2.1.4)$$

with  $\varepsilon_q = \hbar^2 q^2 / 2\mu$  and a phase shift  $\delta$ . The normalizations also differ,

$$\int_0^\infty dr P_{v\ell}(r) P_{v\ell}(r) = \begin{cases} \delta_{n'n} & , \text{ bound states} \\ \delta(\varepsilon' - \varepsilon) & , \text{ continuum states} \end{cases} \quad (2.1.5)$$

The continuum state normalization is not standardized and can include additional constants in Eq. (2.1.5). Alternatively, a  $q$ -scale normalization is often used

$$\int_0^\infty dr P_{q\ell}(r) P_{q\ell}(r) = \delta(q' - q) \quad (2.1.6)$$

and

$$P_{q\ell}(r) = \sqrt{\frac{\hbar^2 q}{\mu}} P_{\varepsilon\ell}(r) \quad (2.1.7)$$

provides the relation between the two normalizations.

## 2.2 Photon ionization in distorted wave approach

The treatment of the photo-effect relies on semi-classical theory with classical radiation fields and first-order time-dependent perturbation theory<sup>19</sup>. A photon of momentum  $\hbar k = \hbar\omega/c$ , with  $c$  the speed of light in vacuum, and energy  $\hbar\omega$  impinges on a bound state of the atom and ejects an electron into a continuum state. The discussion is limited to nonrelativistic electrons; thus, the photon energies are confined to be much smaller than the electron rest energy. The threshold energy for ionization is determined by the binding energy of the bound electron.

The interaction coupling a monochromatic photon beam and the electron is<sup>19</sup>

$$\Phi(\omega, t) = -\frac{e}{\mu c} e^{-i(\vec{k}\cdot\vec{r} + \omega t)} \vec{A}_o \cdot \vec{p} \quad (2.2.1)$$

with  $\vec{p}$  the electron linear momentum operator and  $e$  the elemental unit of electric charge. The interaction assumes the Coulomb gauge where the vector potential satisfies  $\vec{\nabla} \cdot \vec{A} = 0$ . The  $A^2$  term is neglected since it has a vanishing matrix elements between the vacuum and a one-photon state; thus, only contributes in second or higher order perturbation theory. Furthermore, the interaction should contain a term with  $e^{i\omega t}$ , but that term satisfies energy conservation for emission whereas the interest here is absorption.

The transition rate between initial and final energy eigenstates  $\alpha$  and  $\beta$  in Eq. (2.1.1) is given by Fermi's Golden Rule<sup>19</sup>,

$$R_{\alpha\beta}^{DW}(\omega) = \frac{2\pi}{\hbar} |\Phi_{\alpha\beta}|^2 \delta(\varepsilon_\beta - \varepsilon_\alpha - \hbar\omega) \quad (2.2.2)$$

with an energy conserving  $\delta$ -function,  $\varepsilon_\nu$  the energy of the  $\nu$  state, and matrix elements

$$\Phi_{\alpha\beta} = \frac{e}{\mu c} \int d\vec{r} P_{\varepsilon_\beta \ell_\beta} (r) Y_{\ell_\beta m_\beta}^* (\hat{r}) e^{i\vec{k}\cdot\vec{r}} \vec{A}_o \cdot \vec{p} P_{\varepsilon_\alpha \ell_\alpha} (r) Y_{\ell_\alpha m_\alpha} (\hat{r}) \quad (2.2.3)$$

Finally, the total ionization rate of the initial bound state  $\alpha$  by a photon with energy  $\hbar\omega$  requires summing over all possible final states,

$$\begin{aligned} R_\alpha^{DW}(\omega) &= \sum_\beta R_{\alpha\beta}^{DW}(\omega) \\ &= \frac{2\pi}{\hbar} \sum_{\ell_\beta m_\beta} \int d\varepsilon_\beta \rho(\varepsilon_\beta) |\Phi_{\alpha\beta}|^2 \delta(\varepsilon_\beta - \varepsilon_\alpha - \hbar\omega) \\ &= \frac{2\pi}{\hbar} \sum_{\ell_\beta m_\beta} |\Phi_{\alpha\beta}|^2 \end{aligned} \quad (2.2.4)$$

where  $\varepsilon_\beta = \varepsilon_\alpha + \hbar\omega$  in  $\Phi_{\alpha\beta}$  and the density of continuum states  $\rho(\varepsilon) = 1$  for the energy-scale normalization in Eq. (2.1.5). This is the standard distorted wave result.

### 3. TSL model

The premise of the TSL method is that, due to collisions with the plasma, the continuum electrons cannot be described by the usual distorted wave. Instead, the final state is a wave packet constructed by a superposition of energy eigenstates<sup>15</sup>. The expression here emends the TSL superposition formula to display explicitly the time and angular momentum dependence,

$$\begin{aligned} \Psi_{q_o \ell m}(\vec{r}, t) &= r^{-1} Y_{\ell m}(\hat{r}) u_{q_o \ell}(r, t) \\ &= r^{-1} Y_{\ell m}(\hat{r}) \frac{1}{A_{q_o}} \int_{q_o}^{\infty} dq f_{q_o}(q) P_{\varepsilon_q \ell}(r) e^{-i\varepsilon_q t/\hbar} \end{aligned} \quad (3.1)$$

defining  $u_{q_o \ell}(r, t)$  with  $A_{q_o}$  a normalization constant. It is emphasized that the model chooses<sup>15,16</sup> an energy-scale normalization for the eigenfunctions in Eq. (3.1) following Meng et al.<sup>20</sup>, which for non-relativistic electrons is the same as Eq. (2.1.5). The coefficients are<sup>15</sup>

$$f_{q_o}(q) = \frac{\Delta/\pi}{(q - q_o)^2 + \Delta^2} \quad (3.2)$$

with  $\Delta$  the half-width at half-maximum due to natural lifetime and electron impact broadening.

The wave packet is re-normalized to unity over the volume<sup>15,16</sup>, which leads to

$$\begin{aligned}
1 &= \int d\vec{r} \left| \Psi_{q_o, \ell m}(\vec{r}, t) \right|^2 = \int_0^\infty dr \left| u_{q_o, \ell}(r, t) \right|^2 \\
&= \left| A_{q_o} \right|^{-2} \int_0^\infty dq' f_{q_o}^*(q') \int_0^\infty dq f_{q_o}(q) e^{i(\varepsilon_{q'} - \varepsilon_q)t/\hbar} \int_0^\infty dr P_{\varepsilon_{q'}, \ell}(r) P_{\varepsilon_q, \ell}(r) \\
&= \frac{\mu}{\hbar^2 A_{q_o}^2} \int_0^\infty \frac{dq}{q} \left[ \frac{\Delta/\pi}{(q - q_o)^2 + \Delta^2} \right]^2
\end{aligned} \tag{3.3}$$

where the energy-scale normalization was used leading to a divergent integral. Therefore, as described<sup>15,16</sup> the TSL model is ill-defined.

### 3.1 Modified TSL superposition

The divergence in Eq. (3.3) is partially a consequence of the missing density of states in the superposition of the TSL wave packet. To proceed, consider the modified superposition where in Eq. (3.1)  $\Psi \rightarrow \hat{\Psi}$  and

$$u_{q_o, \ell}(r, t) \rightarrow \hat{u}_{q_o, \ell}(r, t) = \frac{1}{C_{q_o}} \int_0^\infty dq f_{q_o}(q) P_{q, \ell}(r) e^{-i\varepsilon_q t/\hbar} \tag{3.1.1}$$

with  $C_{q_o}$  a normalization constant. This is a plausible alternative to Eq. (3.1) making a minor correction to the original TSL description: Change from energy- to  $q$ -scale normalization. The re-normalization of the wave packet now gives,

$$\begin{aligned}
C_{q_o}^2 &= \int_0^\infty dq \left[ \frac{\Delta/\pi}{(q - q_o)^2 + \Delta^2} \right]^2 \\
&= \frac{1}{4\pi\Delta} \left\{ 1 + \frac{2}{\pi} \left[ \frac{\delta_o}{1 + \delta_o^2} + \text{Tan}^{-1}(\delta_o^{-1}) \right] \right\}
\end{aligned} \tag{3.1.2}$$

where  $\delta_o = \Delta/q_o$ .

The wave packet is not stationary but is readily shown to satisfy the time-dependent Schrodinger equation. It has stationary expectation values for time independent operators. As an example, for  $H$  the spherically symmetric Hamiltonian leading to Eq. (2.1.2),



$$\begin{aligned}
\langle H \rangle &= \int d\vec{r} \hat{\Psi}_{q_o \ell m}^*(\vec{r}, t) H \hat{\Psi}_{q_o \ell m}(\vec{r}, t) \\
&= \frac{\hbar^2}{2\mu_o} \int_0^\infty dq q^2 \left| \frac{f_{q_o}(q)}{C_{q_o}} \right|^2 \\
&= \frac{\hbar^2 q_o^2}{2\mu} (1 + \delta_o^2)
\end{aligned} \tag{3.1.3}$$

Note that even though the coefficient in Eq. (3.2) peaks at  $q = q_o$ , the wave packet energy expectation value is not  $\hbar^2 q_o^2 / 2\mu$ . Consequently, the ionization corresponds on average to photon energy

$$\hbar \hat{\omega} = \frac{\hbar^2 q_o^2}{2\mu} (1 + \delta_o^2) - \varepsilon_\alpha \tag{3.1.4}$$

rather than

$$\hbar \omega = \frac{\hbar^2 q_o^2}{2m} - \varepsilon_\alpha \tag{3.1.5}$$

The reader should note that the energy eigenstates in the TSL superposition are not eigenstates of  $q$ , which is related to the energy but is not the state momentum except for the case of plane waves. Also, the average ‘‘momentum’’ for the modified TSL wave packet is given by

$$\int_0^\infty dq q \left| \frac{f_{q_o}(q)}{C_{q_o}} \right|^2 = q_o \left\{ 1 + \frac{\delta_o^3}{\delta_o + (1 + \delta_o^2) \left[ \frac{\pi}{2} + \text{Tan}^{-1}(\delta_o^{-1}) \right]} \right\} \tag{3.1.6}$$

Thus, the interpretation of the superposition in the TSL model is unclear.

### 3.2 Photon ionization in modified TSL approach

Using the manipulations leading to Fermi’s Golden Rule, it is readily shown that the transition rate for ionization of bound state  $\alpha$  to a modified TSL wave packet by a photon of energy  $\hbar \omega$  is

$$R_{\alpha\beta}^{TSL}(\omega) = \frac{2\pi}{\hbar} |\Phi_{\alpha\beta}|^2 \left| \frac{f_{q_o}(q_\beta)}{C_{q_o}} \right|^2 \tag{3.2.1}$$

and again  $\varepsilon_\beta = \varepsilon_\alpha + \hbar \omega$  in  $\Phi_{\alpha\beta}$ . That is, the result replaces the  $\delta$ -function in the Golden Rule with the weight of the eigenstate  $\beta$  in the superposition. As a result, wave packets with different

$q_o$  values can provide final states for the transition and the total transition rate sums over all possible final wave packets,

$$\begin{aligned} R_{\alpha}^{TSL}(\omega) &= R_{\alpha}^{DW}(\omega) \int_0^{\infty} dq_o \left| \frac{f_{q_o}(q)}{C_{q_o}} \right|^2 \\ &= R_{\alpha}^{DW}(\omega) I\left(\frac{\Delta}{q_{\beta}}\right) \end{aligned} \quad (3.2.2)$$

which defines the dimensionless integral  $I(x)$  and  $R_{\alpha}^{DW}$  is given by Eq. (2.2.4).

Inserting Eqs. (3.2) and (3.1.2) together with the change of variable  $y = \Delta/q_o$  get

$$I(x) = \frac{4}{\pi} \int_0^{\infty} dy \frac{y^2(1+y^2)}{\left\{1+y^2 + \frac{2}{\pi} \left[ y + (1+y^2) \text{Tan}^{-1}(y^{-1}) \right] \right\} \left\{ y^2 + \left(1 - \frac{y}{x}\right)^2 \right\}^2} \quad (3.2.3)$$

The integral is computed numerically and displayed in Fig. 1. Consequently, the total ionization rate for the modified wave packet is given by

$$R_{\alpha}^{TSL}(\omega) \approx R_{\alpha}^{DW}(\omega) \quad (3.2.4)$$

for values of  $\Delta/q < 0.2$  reproducing the distorted wave result. For larger values of  $\Delta/q$  (expected for more strongly coupled plasmas) there is at most a 5% increase in the TSL total ionization rate. Interestingly, for  $\Delta/q > 2$  the TSL wave packet reduces the total rate relative to the distorted wave approach with asymptotic limit  $I(x \rightarrow \infty) = \ln 2$ .

#### 4. Summary

Fundamental features of the transient space localization (TSL) model<sup>15</sup> were examined. The method relies on the same cross-section formulas as in the conventional models. The novelty is a replacement of the final continuum energy eigenstates with wave packets to account for plasma effects on the ejected electron. This, however, is an *ad hoc* approximation. Recall that the line shape function involves stationary energy eigenstates of the system, which were approximated by a one-electron picture. A systematic approach to introduce relaxation to those approximate states may well consider expressing the line shape in terms of correlation functions together with a perturbation treatment of collisions as done in spectral line broadening by plasmas<sup>21</sup>. It is

emphasized that such treatments lead to line shifts and widths but do not impact the overall strength of the transition.

The TSL model<sup>15,16</sup> was shown to contain a fundamental theoretical impasse. It was also shown that a plausible minor modification to the TSL model to remove unphysical divergences yields at most a 5% enhancement to the photon ionization cross-sections well below that necessary to resolve the extant discrepancies between experimental and theoretical results. Moreover, for very strongly coupled plasmas it reduces the photon ionization cross-section. Consequently, it is unclear how the TSL model generates enhanced cross-sections.

### **Acknowledgments**

Thanks are due to J.E. Bailey for suggesting the work. The work performed under the auspices of the U.S. Department of Energy by Lawrence Livermore National Laboratory under Contract DE-AC52-07NA27344 as well as the US Department of Energy's National Nuclear Security Administration under Contract No. DE-NA-0003525.

## References

1. Bailey, J.E. et al. Iron-Plasma transmission measurement at temperatures above 150 eV, *Phys. Rev. Lett.* **99**, 265002 (2007)
2. Bailey, J.E. et al. Higher than predicted measurement of iron opacity at solar interior temperatures, *Nature* **517**, 56-59 (2015)
3. Basu, S. & Antia, H.M., Helioseismology and solar abundances, *Phys. Rep.* **457**, 217-283 (2008)
4. Nagayama, T. et al. Systematic study of L-shell opacity at stellar interior temperatures, *Phys. Rev. Lett.* **122**, 235001 (2019)
5. Fontes, C.J. et al. Relativistic opacities for astrophysical applications, *High Energy Density Phys.* **16**, 53-59 (2015)
6. Pain, J.-C. A note on the contribution of multi-photon processes to radiative opacity, *High Energy Density Phys.* **26**, 23-25 (2018)
7. Kruse, M.K.G. & Iglesias, C.A. Two-photon absorption framework for plasma transition experiments, *High Energy Density Phys.* **31**, 38-46 (2019) and references therein
8. Kruse, M.K.G. & Iglesias, C.A. Two-photon absorption ionization in solar opacity experiments, *High Energy Density Phys.* **41**, 100976 (2021)
9. Nahar, S.N. & Pradhan, A.K., Large enhancement in high-energy photoionization of Fe XVII and missing continuum plasma opacity *Phys. Rev. Lett.* **116**, 235003 (2016)
10. Blancard, C. et al. Comment on “Large enhancement in high-energy photoionization of Fe XVII and missing continuum plasma opacity,” *Phys. Rev. Lett.* **117**, 249501(2016)
11. Iglesias, C.A. & Hansen, S.B. Fe XVII opacity at solar interior conditions, *Astrophys. J.* **835**, 284 (2017)
12. Pain, J.-C. & Gilleron, F. Accounting for highly excited states in detailed opacity calculations, *High Energy Density Phys.* **15**, 30-42 (2015)
13. Krief, M., Feigel, A. & Gazit, D. Line broadening and the solar opacity problem, *Astrophys. J.* **824**, 98 (2016)
14. Iglesias, C.A. Enigmatic photon absorption in plasmas near solar interior conditions, *High Energy Density Phys.* **15**, 4-7 (2015)
15. Liu, P. et al. Transient space localization of electrons ejected from continuum atomic processes in hot dense plasma, *Commun. Phys.* **95**, 1-7(2018)
16. Zeng, J. et al., Electron localization enhanced photon absorption for the missing opacity in solar interior, *Sci. China-Phys. Mech. Astron* **65**, 233011(2022)
17. McQuarrie, D.A., *Statistical Mechanics* (Harper & Row, New York, 1976)

18. Cowan, R.D., *The Theory of Atomic Structure and Spectra* (University of California Press, Berkeley, 1981)
19. Gottfried, K., *Quantum Mechanics Volume I: Fundamentals* (W.A. Benjamin, N.Y., 1966)
20. Meng, X-J, Zhu, X.R., Tian, M.F., Jiang, M.H. & Wang, Z.G. Free or quasi-free electronic density of states in a confined atom, *Chin. Phys. Lett.* **22**, 310-313 (2005)
21. Gigosos, M.A. Stark broadening models for plasma diagnostics *J. Phys. D* **47**, 343001 (2014) and references therein

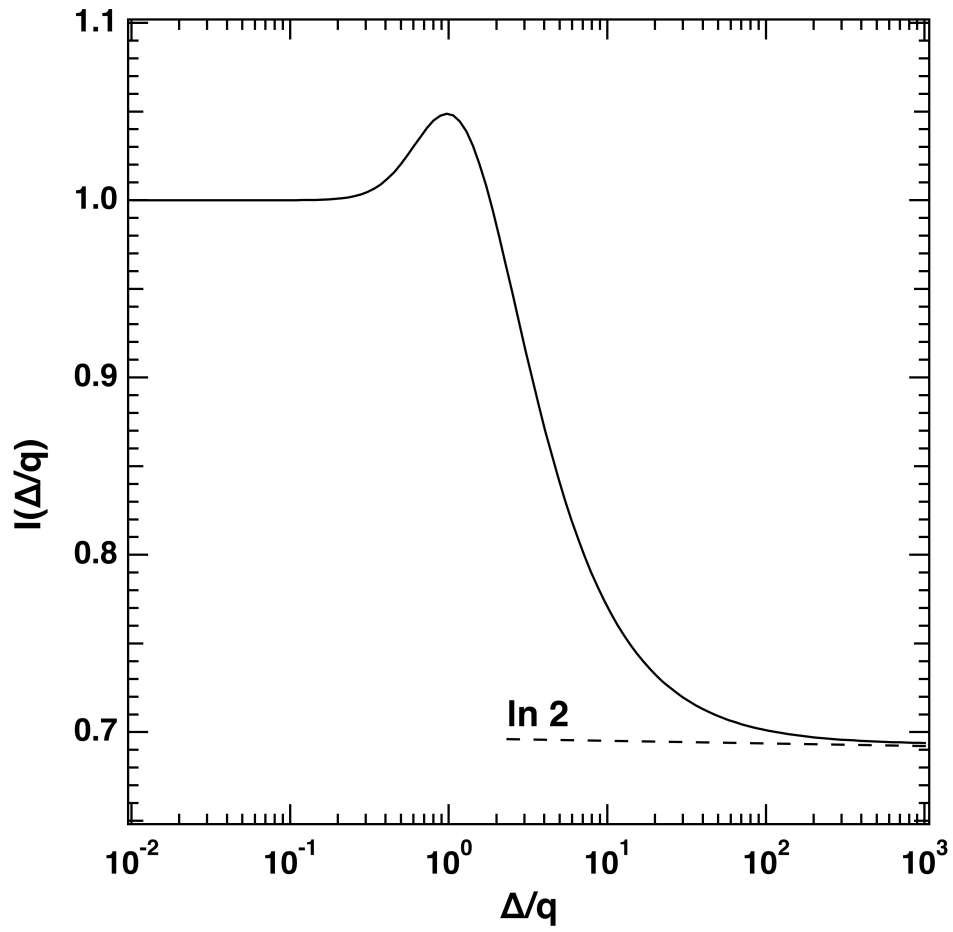


Fig.1 – Plot of integral  $I(\Delta/q)$  as a function of  $\Delta/q$ .